

Probing Few-Body Nuclear Dynamics via ^3H and ^3He ($e,e'p$)pn Cross-Section Measurements

R. Cruz-Torres,^{1,*} D. Nguyen,^{1,2,*} F. Hauenstein,³ A. Schmidt,¹ S. Li,⁴ D. Abrams,⁵ H. Albataineh,⁶ S. Alsalmi,⁷ D. Androic,⁸ K. Aniol,⁹ W. Armstrong,¹⁰ J. Arrington,¹⁰ H. Atac,¹¹ T. Averett,¹² C. Ayerbe Gayoso,¹² X. Bai,⁵ J. Bane,¹³ S. Barcus,¹² A. Beck,¹ V. Bellini,¹⁴ F. Benmokhtar,¹⁵ H. Bhatt,¹⁶ D. Bhetuwal,¹⁶ D. Biswas,¹⁷ D. Blyth,¹⁰ W. Boeglin,¹⁸ D. Bulumulla,³ A. Camsonne,¹⁹ J. Castellanos,¹⁸ J.-P. Chen,¹⁹ E. O. Cohen,²⁰ S. Covrig,¹⁹ K. Craycraft,¹³ B. Dongwi,¹⁷ M. Duer,²⁰ B. Duran,¹¹ D. Dutta,¹⁶ E. Fuchey,²¹ C. Gal,⁵ T. N. Gautam,¹⁷ S. Gilad,¹ K. Gnanvo,⁵ T. Gogami,²² J. Golak,²³ J. Gomez,¹⁹ C. Gu,⁵ A. Habarakada,¹⁷ T. Hague,²⁴ O. Hansen,¹⁹ M. Hattawy,¹⁰ O. Hen,^{1,†} D. W. Higinbotham,¹⁹ E. Hughes,²⁵ C. Hyde,³ H. Ibrahim,²⁶ S. Jian,⁵ S. Joosten,¹¹ H. Kamada,²⁷ A. Karki,¹⁶ B. Karki,²⁸ A. T. Katramatou,²⁴ C. Keppel,¹⁹ M. Khachatryan,³ V. Khachatryan,²⁹ A. Khanal,¹⁸ D. King,³⁰ P. King,²⁸ I. Korover,³¹ T. Kutz,²⁹ N. Lashley-Colthirst,¹⁷ G. Laskaris,¹ W. Li,³² H. Liu,²⁵ N. Liyanage,⁵ P. Markowitz,¹⁸ R. E. McClellan,¹⁹ D. Meekins,¹⁹ S. Mey-Tal Beck,¹ Z.-E. Meziani,^{10,33} R. Michaels,¹⁹ M. Mihovilović,^{34,35,36} V. Nelyubin,⁵ N. Nuruzzaman,¹⁷ M. Nycz,²⁴ R. Obrecht,²¹ M. Olson,³⁷ L. Ou,¹ V. Owen,¹² B. Pandey,¹⁷ V. Pandey,³⁸ A. Papadopoulou,¹ S. Park,²⁹ M. Patsyuk,¹ S. Paul,¹² G. G. Petratos,²⁴ E. Piassetzky,²⁰ R. Pomatsalyuk,³⁹ S. Premathilake,⁵ A. J. R. Puckett,²¹ V. Punjabi,⁴⁰ R. Ransome,⁴¹ M. N. H. Rashad,³ P. E. Reimer,¹⁰ S. Riordan,¹⁰ J. Roche,²⁸ M. Sargsian,¹⁸ N. Santiesteban,⁴ B. Sawatzky,¹⁹ E. P. Segarra,¹ B. Schmookler,¹ A. Shahinyan,⁴² S. Širca,^{34,43} R. Skibiński,²³ N. Sparveris,³³ T. Su,²⁴ R. Suleiman,¹⁹ H. Szumila-Vance,¹⁹ A. S. Tadepalli,⁴¹ L. Tang,¹⁹ W. Tireman,⁴⁴ K. Topolnicki,²³ F. Tortorici,¹⁴ G. Urciuoli,⁴⁵ L. B. Weinstein,³ H. Witała,²³ B. Wojtsekhowski,¹⁹ S. Wood,¹⁹ Z. H. Ye,¹⁰ Z. Y. Ye,⁴⁶ and J. Zhang²⁹

(Jefferson Lab Hall A Tritium Collaboration)

¹Massachusetts Institute of Technology, Cambridge, Massachusetts 02139, USA

²University of Education, Hue University, Hue City, Vietnam

³Old Dominion University, Norfolk, Virginia 23529, USA

⁴University of New Hampshire, Durham, New Hampshire 03824, USA

⁵University of Virginia, Charlottesville, Virginia 22904, USA

⁶Texas A & M University, Kingsville, Texas 78363, USA

⁷King Saud University, Riyadh 11451, Kingdom of Saudi Arabia

⁸University of Zagreb, 10000 Zagreb, Croatia

⁹California State University, Los Angeles, California 90032, USA

¹⁰Physics Division, Argonne National Laboratory, Lemont, Illinois 60439, USA

¹¹Temple University, Philadelphia, Pennsylvania 19122, USA

¹²The College of William and Mary, Williamsburg, Virginia 23185, USA

¹³University of Tennessee, Knoxville, Tennessee 37966, USA

¹⁴INFN Sezione di Catania, 95123 Catania, Italy

¹⁵Duquesne University, Pittsburgh, Pennsylvania 15282, USA

¹⁶Mississippi State University, Mississippi 39762, USA

¹⁷Hampton University, Hampton, Virginia 23669, USA

¹⁸Florida International University, Miami, Florida 33199, USA

¹⁹Jefferson Lab, Newport News, Virginia 23606, USA

²⁰School of Physics and Astronomy, Tel Aviv University, Tel Aviv 69978, Israel

²¹University of Connecticut, Storrs, Connecticut 06269, USA

²²Tohoku University, Sendai, Miyagi 980-8577, Japan

²³M. Smoluchowski Institute of Physics, Jagiellonian University, PL-30348 Kraków, Poland

²⁴Kent State University, Kent, Ohio 44240, USA

²⁵Columbia University, New York, New York 10027, USA

²⁶Cairo University, 12613 Cairo, Egypt

²⁷Department of Physics, Faculty of Engineering, Kyushu Institute of Technology, Kitakyushu 804-8550, Japan

²⁸Ohio University, Athens, Ohio 45701, USA

²⁹Stony Brook, State University of New York, New York 11794, USA

³⁰Syracuse University, Syracuse, New York 13244, USA

³¹Nuclear Research Center-Negev, Beer-Sheva, Israel

³²University of Regina, Regina, SK S4S 0A2, Canada

³³Columbia University, New York, New York 10027, USA

³⁴University of Ljubljana, 1000 Ljubljana, Slovenia³⁵Faculty of Mathematics and Physics, Jožef Stefan Institute, Ljubljana, Slovenia³⁶Institut für Kernphysik, Johannes Gutenberg-Universität Mainz, DE-55128 Mainz, Germany³⁷Saint Norbert College, De Pere, Wisconsin 54115, USA³⁸Department of Physics, University of Florida, Gainesville, Florida 32611, USA³⁹Institute of Physics and Technology, Kharkov 61108, Ukraine⁴⁰Norfolk State University, Norfolk, Virginia 23504, USA⁴¹Rutgers University, New Brunswick, New Jersey 08901, USA⁴²Yerevan Physics Institute, 0036 Yerevan, Armenia⁴³Faculty of Mathematics and Physics, Jožef Stefan Institute, SI-1000, Ljubljana, Slovenia⁴⁴Northern Michigan University, Marquette, Michigan 49855, USA⁴⁵INFN, 00185 Rome, Italy⁴⁶University of Illinois-Chicago, Chicago, Illinois 60607, USA

(Received 29 January 2020; revised manuscript received 12 March 2020; accepted 30 April 2020; published 26 May 2020)

We report the first measurement of the $(e, e'p)$ three-body breakup reaction cross sections in helium-3 (^3He) and tritium (^3H) at large momentum transfer [$\langle Q^2 \rangle \approx 1.9 \text{ (GeV}/c)^2$] and $x_B > 1$ kinematics, where the cross section should be sensitive to quasielastic (QE) scattering from single nucleons. The data cover missing momenta $40 \leq p_{\text{miss}} \leq 500 \text{ MeV}/c$ that, in the QE limit with no rescattering, equals the initial momentum of the probed nucleon. The measured cross sections are compared with state-of-the-art *ab initio* calculations. Overall good agreement, within $\pm 20\%$, is observed between data and calculations for the full p_{miss} range for ^3H and for $100 \leq p_{\text{miss}} \leq 350 \text{ MeV}/c$ for ^3He . Including the effects of rescattering of the outgoing nucleon improves agreement with the data at $p_{\text{miss}} > 250 \text{ MeV}/c$ and suggests contributions from charge-exchange (SCX) rescattering. The isoscalar sum of ^3He plus ^3H , which is largely insensitive to SCX, is described by calculations to within the accuracy of the data over the entire p_{miss} range. This validates current models of the ground state of the three-nucleon system up to very high initial nucleon momenta of $500 \text{ MeV}/c$.

DOI: [10.1103/PhysRevLett.124.212501](https://doi.org/10.1103/PhysRevLett.124.212501)

Understanding the structure and properties of nuclear systems is a formidable challenge with implications ranging from the formation of elements in the Universe to their application in laboratory measurements of fundamental interactions. Due to the complexity of the strong nuclear interaction, nuclear systems are often described using effective models that are based on various levels of approximations. Testing and benchmarking such approximations is a high priority of modern nuclear physics research.

Measurements of high-energy quasielastic (QE) electron scattering serve a unique role in this endeavor as they can be particularly sensitive to ground state properties of nuclei [1]. However, in many studies this sensitivity is reduced by the lack of exact nuclear ground-state calculations and by the contribution of non-QE processes to the measured cross sections. Calculations of non-QE contributions are highly model dependent and can change the resulting cross sections dramatically, hindering the interpretation of measurements in terms of the nuclear ground state [2].

Studies of the three nucleon system can avoid these issues as (i) their ground states are exactly calculable from nuclear-interaction models, and (ii) proper choice of kinematics can suppress cross section contributions from non-QE processes, allowing one to directly relate measured cross sections to the ground-state momentum distribution.

Thus electron scattering studies of helium-3 (^3He) and tritium (^3H) nuclei can serve as a precision test of modern nuclear theory [3].

While vast amounts of modern electron scattering data on ^3He exist [4–12], ^3H data are very sparse due to the safety limitations associated with placing a radioactive tritium target in a high-current electron beam. Current world data dates back to the early 1960s [13–16] and late 1980s [17–22].

This Letter reports the first electron scattering cross sections on ^3H to be published in over 30 years. Specifically, we study the distributions of protons in ^3He and in ^3H using measurements of high-energy QE proton knockout reactions in comparison with predictions of state-of-the-art *ab initio* calculations to test their modeling of the three-nucleon ground state up to very large initial momenta. The simultaneous measurement of both ^3He and $^3\text{H}(e, e'p)$ cross sections, at the kinematics of our experiment, places stringent constraints on the possible contribution of non-QE reaction mechanisms to our measurement, thereby improving the equivalence between the measured missing momenta and initial nucleon momenta and increasing its sensitivity to the properties of the ^3He and ^3H ground states.

Our measured cross sections are well described by theoretical calculations to about 20%, without the need to

include non-QE processes. This is a great improvement over recent ${}^3\text{He}(e, e'p)$ measurements [5] that were dominated by non-QE processes and were therefore significantly less sensitive to its ground state, especially at large missing momentum. Our ${}^3\text{H}$ data is better described by calculations than ${}^3\text{He}$. Including leading nucleon rescattering improves the agreement between the calculations and the data. The remaining small difference between data and theory has the opposite trend for ${}^3\text{He}$ and ${}^3\text{H}$, which could suggest residual contributions from single charge exchange (SCX) processes. The effects of SCX are largely suppressed in the isoscalar sum of ${}^3\text{He} + {}^3\text{H}$ cross sections, which is described by calculations to within the accuracy of our data. We thus confirm modeling of the three-nucleon system up to very high nucleon momenta of 500 MeV/c.

The experiment ran in 2018 in Hall A of the Thomas Jefferson National Accelerator Facility. It used the two high-resolution spectrometers (HRSs) [23] and a 20 μA electron beam at 4.326 GeV incident on one of four identical 25-cm-long gas target cells filled with hydrogen ($70.8 \pm 0.4 \text{ mg/cm}^2$), deuterium ($142.2 \pm 0.8 \text{ mg/cm}^2$), helium-3 ($53.4 \pm 0.6 \text{ mg/cm}^2$), and tritium ($85.1 \pm 0.8 \text{ mg/cm}^2$) [24]. To minimize systematic uncertainties between measurements, the HRS were not moved when changing among the targets, which were installed on a linear motion target ladder.

Each HRS consisted of three quadrupole magnets for focusing and one dipole magnet for momentum analysis, followed by a detector package consisting of a pair of vertical drift chambers used for tracking and two scintillation counter planes that provided timing and trigger signals. A CO_2 Cherenkov detector placed between the scintillators and a lead-glass calorimeter placed after them were used for particle identification. This configuration is slightly updated with respect to the one in Ref. [23].

Scattered electrons were detected in the left-HRS, positioned at central momentum and angle of $|\vec{p}'_e| = 3.543 \text{ GeV}/c$ and $\theta_e = 20.88^\circ$, giving a central four-momentum transfer $Q^2 = \vec{q}^2 - \omega^2 = 2.0 \text{ (GeV}/c)^2$ (where the momentum transfer is $\vec{q} = \vec{p}_e - \vec{p}'_e$), energy transfer $\omega = E_{\text{beam}} - |\vec{p}'_e| = 0.78 \text{ GeV}$, and $x_B \equiv (Q^2/2m_p\omega) = 1.4$ (where m_p is the proton mass). Knocked-out protons were detected in the right-HRS at two central settings of $(\theta_p, p_p) = (48.82^\circ, 1.481 \text{ GeV}/c)$, and $(58.50^\circ, 1.246 \text{ GeV}/c)$ corresponding to low- p_{miss} ($40 \leq p_{\text{miss}} \leq 250 \text{ MeV}/c$) and high- p_{miss} ($250 \leq p_{\text{miss}} \leq 500 \text{ MeV}/c$), respectively, where $\vec{p}_{\text{miss}} = \vec{p}_p - \vec{q}$. The exact electron kinematics for each p_{miss} bin varied within the spectrometer acceptances.

In the plane wave impulse approximation (PWIA) for QE scattering, where a single exchanged photon is absorbed on a single proton and the knocked-out proton does not reinteract as it leaves the nucleus, the cross section is proportional to the spectral function, the probability of finding a proton in the nucleus with initial momentum \vec{p}_i and separation energy E_i . The momentum distribution is

then the integral of the spectral function over E_i : $n(p_i) = \int S(p_i, E_i) dE_i$. In PWIA, the missing momentum and energy equal the initial momentum and separation energy of the knocked-out nucleon: $\vec{p}_i = \vec{p}_{\text{miss}}$, $E_i = E_{\text{miss}}$, where $E_{\text{miss}} = \omega - T_p - T_{A-1}$, $T_{A-1} = (\omega + m_A - E_p) - \sqrt{(\omega + m_A - E_p)^2 - |\vec{p}_{\text{miss}}|^2}$ is the reconstructed kinetic energy of the residual $A - 1$ system. T_p and E_p are the measured kinetic and total energies of the outgoing proton.

Non-QE reaction mechanisms that lead to the same measured final state also contribute to the cross section, complicating this simple picture. Such mechanisms include rescattering of the struck nucleon (final-state interactions or FSI), meson-exchange currents (MEC), and exciting isobar configurations (IC). In addition, relativistic effects can be significant [25–27].

The kinematics of our measurement were chosen to reduce contributions from such non-QE reaction mechanisms. For high- Q^2 reactions, the effects of FSI were shown to be reduced by choosing kinematics where the angle between $\vec{p}_{\text{recoil}} = -\vec{p}_{\text{miss}}$ and \vec{q} is $\theta_{rq} \lesssim 40^\circ$, which also corresponds to $x_B \geq 1$ [28–34]. Additionally MEC and IC were shown to be suppressed for $Q^2 > 1.5 \text{ (GeV}/c)^2$ and $x_B > 1$ [29,35].

The data analysis follows that previously reported in Ref. [36] for the ${}^3\text{He}/{}^3\text{H}(e, e'p)$ cross section ratio extraction. We selected electrons by requiring that the particle deposits more than half of its energy in the calorimeter: $E_{\text{cal}}/|\vec{p}| > 0.5$. We selected $(e, e'p)$ coincidence events by placing $\pm 3\sigma$ cuts around the relative electron and proton event times and the relative electron and proton reconstructed target vertices (corresponding to a $\pm 1.2 \text{ cm}$ cut). Due to the low experimental luminosity, the random coincidence event rate was negligible. We discarded a small number of runs with anomalous event rates.

Measured electrons were required to originate within the central $\pm 9 \text{ cm}$ of the gas target to exclude events originating from the target walls. By measuring scattering from an empty-cell-like target we determined that the target cell wall contribution to the measured $(e, e'p)$ event yield was negligible ($\ll 1\%$).

To avoid the acceptance edges of the spectrometer, we only analyzed events that were detected within $\pm 4\%$ of the central spectrometer momentum, and $\pm 27.5 \text{ mrad}$ in in-plane angle and $\pm 55.0 \text{ mrad}$ in out-of-plane angle relative to the center of the spectrometer acceptance. We further required $\theta_{rq} < 37.5^\circ$ to minimize the effect of FSI and, in the high- p_{miss} kinematics, $x_B > 1.3$ to further suppress non-QE events.

The spectrometers were calibrated using sieve slit measurements to define scattering angles and by measuring the kinematically overconstrained exclusive ${}^1\text{H}(e, e'p)$ and ${}^2\text{H}(e, e'p)n$ reactions. The ${}^1\text{H}(e, e'p)$ reaction p_{miss} resolution was better than $9 \text{ MeV}/c$. We verified the absolute

luminosity normalization by comparing the measured elastic ${}^1\text{H}(e, e')$ yield to a parametrization of the world data [37]. We also found excellent agreement between the elastic ${}^1\text{H}(e, e'p)$ and ${}^1\text{H}(e, e')$ rates, confirming that the coincidence trigger performed efficiently.

One significant difference between ${}^3\text{He}(e, e'p)$ and ${}^3\text{H}(e, e'p)$ stems from their possible final states. The ${}^3\text{H}(e, e'p)$ reaction can only result in a three-body pnn continuum state, while ${}^3\text{He}$ can break up into either a two-body pd state or a three-body ppn continuum state. To allow for a more detailed comparison of the two nuclei we only considered three-body breakup reactions by requiring $E_{\text{miss}} > 8$ MeV (i.e., above the ${}^3\text{He}$ two-body breakup peak).

The cross section was calculated from the $(e, e'p)$ event yield in a given $(p_{\text{miss}}, E_{\text{miss}})$ bin as:

$$\frac{d^6\sigma(p_{\text{miss}}, E_{\text{miss}})}{dE_e dE_p d\Omega_e d\Omega_p} = \frac{\text{Yield}(p_{\text{miss}}, E_{\text{miss}})}{Ct(\rho/A)bV_B C_{\text{Rad}} C_{\text{BM}}}, \quad (1)$$

where C is the total accumulated beam charge, t is the live time fraction in which the detectors are able to collect data, $A = 3$ is the target atomic mass, ρ is the nominal areal density of the gas in the target cell, and b is a correction factor to account for changes in the target density caused by local beam heating. b was determined by measuring the beam current dependence of the inclusive event yield [24]. V_B is a factor that accounts for the detection phase space and acceptance correction for the given $(p_{\text{miss}}, E_{\text{miss}})$ bin and C_{Rad} and C_{BM} are the radiative and bin migration corrections, respectively. The ${}^3\text{H}$ event yield was also corrected for the radioactive decay of $2.78 \pm 0.18\%$ of the target ${}^3\text{H}$ nuclei to ${}^3\text{He}$ in the six months between when the target was filled and when the experiment was conducted.

We used the SIMC [38] spectrometer simulation package to simulate our experiment to calculate the V_B , C_{Rad} , and C_{BM} terms in Eq. (1), and to compare the measured cross section with theoretical calculations. SIMC generates $(e, e'p)$ events with the addition of radiation effects over a wide phase space, propagates the generated events through a spectrometer model to account for acceptance and resolution effects, and then weights each accepted event by a model cross section calculated for the original kinematics of that specific event. The weighted events are subsequently analyzed as the data and can be used to compare between the data and different model cross section predictions.

We considered two PWIA cross section models: (i) Faddeev-formulation-based calculations by J. Golak *et al.* [3,39,40] that either include or exclude the continuum interaction between the two spectator nucleons (FSI₂₃), labeled Cracow and Cracow-PW, respectively, and (ii) a factorized calculation using the ${}^3\text{He}$ spectral function of C. Ciofi degli Atti and L. P. Kaptari including FSI₂₃ [41] and

the σ_{cc1} electron off-shell nucleon cross section [42], labeled CK + CC1. Due to the lack of ${}^3\text{H}$ proton spectral functions, we assumed isospin symmetry and used the ${}^3\text{He}$ neutron spectral function for the ${}^3\text{H}(e, e'p)$ simulation. In addition, the Cracow calculation used the CD-Bonn nucleon-nucleon potential [43] and CK used AV18 [44]. To make consistent comparisons within this Letter, we rescaled the CK calculation for each nucleus by the ratio of the proton momentum distribution obtained with CD-Bonn relative to that obtained with AV18 based on calculations in Ref. [45].

We corrected the ${}^3\text{He}$ and ${}^3\text{H}$ cross sections for radiation and bin migration effects using SIMC and the CK + CC1 cross section model that reproduces the p_{miss} dependence of the measured cross section well. Due to the excellent resolution of the HRS, bin migration effects were very small. Radiation effects were also small for ${}^3\text{H}$ ($\lesssim 20\%$), but significant for ${}^3\text{He}$ at low- p_{miss} due to two-body breakup events that reconstructed to $E_{\text{miss}} > 8$ MeV due to radiation. Since the ${}^3\text{He}$ cross section at high E_{miss} is dominated by radiative effects, we required $E_{\text{miss}} < 50$ and 80 MeV for the low- and high- p_{miss} kinematics, respectively.

We then integrated the two dimensional experimental and theoretical cross sections, $\sigma(p_{\text{miss}}, E_{\text{miss}})$, over E_{miss} to get the cross sections as a function of p_{miss} .

To facilitate comparison with future theoretical calculations, we bin-centered the resulting cross sections, using the ratio of the point theoretical cross section to the acceptance-averaged theoretical cross section. We calculated the point theoretical cross section by summing the cross section evaluated at the central $(\langle Q^2 \rangle, \langle x_B \rangle)$ values over the seven E_{miss} bins for that p_{miss} as follows:

$$\begin{aligned} \sigma_{\text{point}}(p_{\text{miss}}) &= \sum_{j=1}^7 \sigma(\langle Q^2 \rangle^j, \langle x_B \rangle^j, p_{\text{miss}}, E_{\text{miss}}^j) \times \Delta E_{\text{miss}}^j, \quad (2) \end{aligned}$$

where j labels the E_{miss} bin and ΔE_{miss}^j is the bin width. We used both the Cracow and CK + CC1 cross section models for this calculation, taking their average as the correction factor and their difference divided by $\sqrt{12}$ as a measure of its 1σ uncertainty. Future calculations can directly compare to our data by calculating the cross section at a small number of points and using Eq. (2), rather than by computationally-intensive integration over spectrometer acceptances.

The point-to-point systematical uncertainties due to the event selection criteria (momentum and angular acceptances, and θ_{r_q} and x_B limits) were determined by repeating the analysis 100 times, selecting each criterion randomly within reasonable limits for each iteration. The systematic uncertainty was taken to be the standard deviation of the resulting distribution cross sections. They range from 1% to

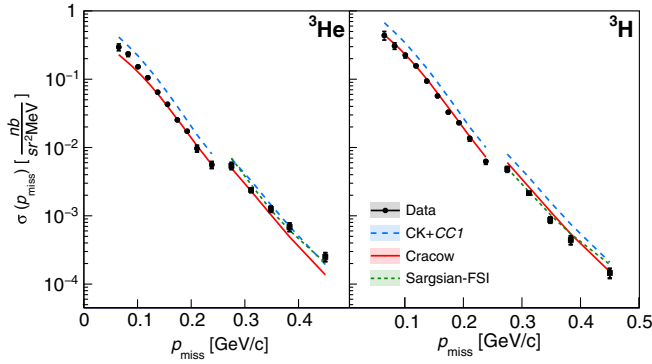


FIG. 1. Absolute cross section as a function of p_{miss} for ${}^3\text{He}$ (left) and ${}^3\text{H}$ (right). The different sets of data points, depicted by black circles and squares, correspond to the cross sections measured in the low- p_{miss} and high- p_{miss} kinematical settings respectively. The lines correspond to cross sections calculated from different theoretical models, Cracow (solid red), CK+CC1 (dashed blue) and Sargsian-FSI (dotted green, $p_{\text{miss}} > 250$ MeV/c only). The different kinematical settings have different average elementary electron-nucleon cross sections and therefore have a different overall scale for both data and calculations.

8% and are typically much smaller than the statistical uncertainties. Additional point-to-point systematics are due to bin-migration, bin-centering, and radiative corrections and range between 0.5% and 3.5%.

The overall normalization uncertainty of our measurement equals 2.7%, and is due to uncertainty in the target density (1.5%), beam-charge measurement run-by-run stability (1%), tritium decay correction (0.15%), and spectrometer detection and trigger efficiencies (2%).

For completeness we also used SIMC to calculate the acceptance-averaged cross sections using both Cracow and CK + CC1 cross section models and compared them to our measured data before any bin-centering corrections. Both models well reproduce the shape of the measured E_{miss} and p_{miss} event distributions. The ratio of the acceptance-averaged experimental to theoretical cross section is similar to the bin-centered ratios shown here.

Figure 1 shows the experimental, bin-centered, ${}^3\text{He}$ and ${}^3\text{H}(e, e'p)$ cross sections as a function of p_{miss} and integrated over E_{miss} from 8 to 50 or 80 MeV for the low- and high- p_{miss} kinematics, respectively. The cross section drops more than a factor of 10^3 from the lowest to highest p_{miss} . The Cracow calculation appears to agree well with measured cross sections for ${}^3\text{He}$ for $p_{\text{miss}} < 350$ MeV/c and for ${}^3\text{H}$ at all p_{miss} , while the CK + CC1 calculation generally overestimates the measured cross sections.

For ease of comparison, Fig. 2 shows the same measured cross sections divided by the PWIA calculations. For ${}^3\text{H}$, the Cracow calculation agrees with the data to about 20%. For ${}^3\text{He}$, the two agree for $100 \leq p_{\text{miss}} \leq 350$ MeV/c but disagree by up to a factor of two for larger and lower p_{miss} .

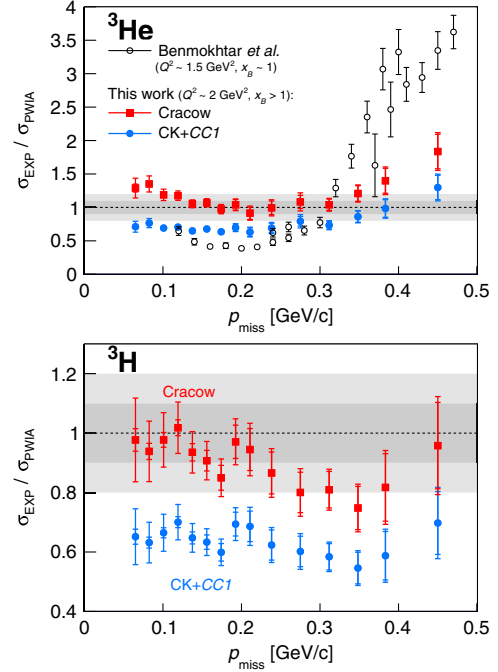


FIG. 2. The ratio of the experimental cross section to different PWIA calculations plotted versus p_{miss} for ${}^3\text{He}(e, e'p)$ (top) and ${}^3\text{H}(e, e'p)$ (bottom). Red squares show the ratio to the Cracow calculation while blue circles show the ratio to the Ciofi-Kaptari spectral-function-based calculations (CK+CC1) (see text for details). Open symbols show the ${}^3\text{He}(e, e'p)$ data of Ref. [5], taken at lower Q^2 and $x \sim 1$ kinematics, compared with the PWIA calculations of Ref. [32,46–48]. The inner and outer bars show the statistical and statistical plus systematic uncertainties, respectively. The shaded regions show 10% and 20% agreement intervals.

For both nuclei the CK + CC1 calculation is higher than the data by about 60%. These results are consistent with our ${}^3\text{He}/{}^3\text{H}$ cross section ratio extracted from the same data [36], which agreed with ratios of cross section calculations and ratios of ground-state momentum distributions up to $p_{\text{miss}} \approx 350$ MeV/c. The unexpected increase in the ${}^3\text{He}/{}^3\text{H}$ cross section ratio at larger p_{miss} now appears to be due to both a decrease in the ${}^3\text{H}(e, e'p)$ and an increase in the ${}^3\text{He}(e, e'p)$ cross sections, relative to PWIA calculations. As explained below, our data suggests that this effect is due to SCX effects.

The most recent ${}^3\text{He}(e, e'p)$ three-body breakup cross section measurements were done at $Q^2 = 1.5$ (GeV/c) 2 and $x_B = 1$ [5], near the expected maximum of struck-proton rescattering. The measured cross sections were lower than PWIA calculations by a factor of ~ 2 for $p_{\text{miss}} < 250$ MeV/c and higher by a factor of ~ 3 for $400 < p_{\text{miss}} < 500$ MeV/c (see Fig. 2). These deviations were described by calculations which included the contribution of non-QE reaction mechanisms, primarily FSI [32,46–48]. The large contribution of such non-QE reaction mechanisms to the measured $(e, e'p)$ cross sections significantly limited their

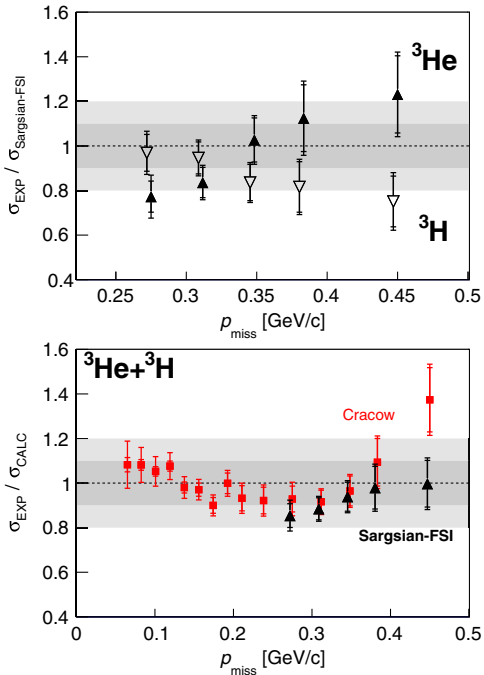


FIG. 3. Top: The ratio of the experimental cross sections to the calculation of Sargsian that includes FSI of the leading nucleon for ${}^3\text{He}$ (filled upright triangles) and ${}^3\text{H}$ (open inverted triangles). Bottom: the ratio of the measured total ${}^3\text{He} + {}^3\text{H}$ cross section to the Cracow PWIA calculation (red squares) and the Sargsian calculation that includes FSI (black triangles). The inner and outer bars show the statistical and statistical plus systematic uncertainties respectively. On both panels the shaded regions show 10% and 20% agreement intervals.

ability to constrain the nucleon distributions at high momenta. These non-QE effects are much smaller in the current measurement due to our choice of kinematics.

In order to estimate the effects of struck-proton rescattering, we also considered a calculation by M. Sargsian [49] which accounts for the FSI of the struck nucleon using the generalized Eikonal approximation [50,51], following the initial PWIA proton knockout. This calculation does not include the continuum interaction between the two spectator nucleons, FSI_{23} , and is therefore only applicable where those effects are small. Comparing the Cracow calculations with and without FSI_{23} showed that its effects decrease rapidly with p_{miss} . We therefore used the Sargsian FSI calculations only at $p_{\text{miss}} \geq 250$ MeV/c. We further verified that using this model for bin centering did not significantly change the correction factors.

See the online Supplemental Material [52] for more details on the kinematics, analysis procedures, and theoretical corrections, and for tables of all measured and calculated cross sections.

Figure 3 (top) shows the ratio of the experimental, bin-centered cross section to the Sargsian FSI calculation for $p_{\text{miss}} > 250$ MeV/c. The FSI calculation generally agrees with the data. The trend of the ratio seems to be opposite for

${}^3\text{He}$ and ${}^3\text{H}$ with the former rising above unity while the latter decreasing below it.

If the high-momentum proton and neutron densities are equal in both ${}^3\text{He}$ and ${}^3\text{H}$, this trend could result from SCX processes which would increase the ${}^3\text{He}(e, e'p)$ cross section, but decrease the ${}^3\text{H}(e, e'p)$ cross section. While further calculations are needed to fully quantify this effect, this equal-density assumption is supported both by *ab initio* calculations [53] and by previous measurements that showed that, at high p_{miss} , electrons scatter primarily off nucleons in np -short-range correlated pairs [54–64]. We can test this, since SCX effects should be suppressed in isoscalar systems due to large cancellations between (n, p) and (p, n) processes. This implies that the isoscalar $A = 3$ cross-section (i.e., ${}^3\text{He} + {}^3\text{H}$) is insensitive to these effects.

The ratio of the measured total isoscalar $A = 3$ cross section of ${}^3\text{He} + {}^3\text{H}$ to the Cracow and Sargsian calculations is shown in Fig. 3(bottom). As expected, both calculations agree with the data to within about $\pm 10\%$, comparable to the accuracy of the data. Due to the QE nature of our measurement, this excellent agreement between our isoscalar data and *ab initio* nuclear theory validates calculations of the $A = 3$ ground state momentum distribution up to extremely high nucleon momenta of about 500 MeV/c.

To conclude, we present new ${}^3\text{He}$ and ${}^3\text{H}(e, e'p)$ cross section measurements, which represent the first new high-energy electron scattering data on tritium in over 30 years. By choosing kinematics specifically to minimize non-quasielastic contributions (high- Q^2 , $x_B > 1$, $\theta_{rq} < 37.5^\circ$), the data are much more directly sensitive to the properties of the $A = 3$ nuclear ground state. PWIA calculations can reproduce the ${}^3\text{He}$ data to within $\pm 20\%$ for $100 \leq p_{\text{miss}} \leq 350$ MeV/c, a significant improvement over previous measurements at $x_B = 1$, and do even better for ${}^3\text{H}$, where they can reproduce the data to $\pm 20\%$ over the entire measured p_{miss} range. A calculation that includes leading nucleon rescattering improves agreement at high p_{miss} , and the residual disagreement has the same sign as would be expected from additional SCX contributions. The isoscalar (${}^3\text{He} + {}^3\text{H}$) cross section agrees remarkably well with QE cross section calculations, validating both the choice of kinematics and calculations of the $A = 3$ ground state up to extremely high nucleon momenta of 500 MeV/c.

These data are a crucial benchmark for few-body nuclear theory and are a necessary, but not sufficient, test of theoretical calculations that are also used in the study of heavier nuclear systems.

We acknowledge the contribution of the Jefferson-Lab target group and technical staff for design and construction of the tritium target and their support running this experiment. We thank C. Ciofi degli Atti and L. Kaptari for the ${}^3\text{He}$ spectral function calculations and M. Sargsian for the FSI calculations. We also thank M. Strikman for many

valuable discussions. This work was supported by the U.S. Department of Energy (DOE) Grant No. DE-AC05-06OR23177 under which Jefferson Science Associates, LLC, operates the Thomas Jefferson National Accelerator Facility, the U.S. National Science Foundation, the Pazi foundation, and the Israel Science Foundation. The Kent State University contribution is supported under Grant No. PHY-1714809 from the U.S. National Science Foundation. The University of Tennessee contribution is supported by Grant No. DE-SC0013615. The work of ANL group members is supported by DOE Grant No. DE-AC02-06CH11357. The contribution of the Cracow group was supported by the Polish National Science Centre under Grants No. 2016/22/M/ST2/00173 and No. 2016/21/D/ST2/01120. The numerical calculations were partially performed on the supercomputer cluster of the JSC, Jülich, Germany. The Temple University group is supported by the DOE Award No. DE-SC0016577.

*These authors contributed equally to this work.

†Contact Author hen@mit.edu

- [1] J. J. Kelly, *Adv. Nucl. Phys.* **23**, 75 (1996).
- [2] W. P. Ford, S. Jeschonnek, and J. W. Van Orden, *Phys. Rev. C* **90**, 064006 (2014).
- [3] J. Golak, R. Skibiński, H. Witała, W. Glöckle, A. Nogga, and H. Kamada, *Phys. Rep.* **415**, 89 (2005).
- [4] I. Sick, *Prog. Part. Nucl. Phys.* **47**, 245 (2001).
- [5] F. Benmokhtar *et al.* (Jefferson Lab Hall A Collaboration), *Phys. Rev. Lett.* **94**, 082305 (2005).
- [6] M. M. Rvachev *et al.* (Jefferson Lab Hall A Collaboration), *Phys. Rev. Lett.* **94**, 192302 (2005).
- [7] E. Long *et al.*, *Phys. Lett. B* **797**, 134875 (2019).
- [8] M. Mihovilovic *et al.* (Jefferson Lab Hall A Collaboration), *Phys. Rev. Lett.* **113**, 232505 (2014).
- [9] M. Mihovilovi *et al.* (Jefferson Lab Hall A Collaboration), *Phys. Lett. B* **788**, 117 (2019).
- [10] Y. W. Zhang *et al.*, *Phys. Rev. Lett.* **115**, 172502 (2015).
- [11] A. Camsonne *et al.*, *Phys. Rev. Lett.* **119**, 162501 (2017); **119**, 209901(A) (2017).
- [12] S. Riordan *et al.*, *Phys. Rev. Lett.* **105**, 262302 (2010).
- [13] H. Collard, R. Hofstadter, A. Johansson, R. Parks, M. Ryneveld, A. Walker, M. R. Yearian, R. B. Day, and R. T. Wagner, *Phys. Rev. Lett.* **11**, 132 (1963).
- [14] L. I. Schiff, H. Collard, R. Hofstadter, A. Johansson, and M. R. Yearian, *Phys. Rev. Lett.* **11**, 387 (1963).
- [15] A. Johansson, *Phys. Rev.* **136**, B1030 (1964).
- [16] T. A. Griffy and R. J. Oakes, *Rev. Mod. Phys.* **37**, 402 (1965).
- [17] K. Dow, *Lect. Notes Phys.* **260**, 346 (1986).
- [18] D. H. Beck, *Lect. Notes Phys.* **260**, 138 (1986).
- [19] D. Beck *et al.*, *Phys. Rev. Lett.* **59**, 1537 (1987).
- [20] K. Dow *et al.*, *Phys. Rev. Lett.* **61**, 1706 (1988).
- [21] F. P. Juster *et al.*, *Phys. Rev. Lett.* **55**, 2261 (1985).
- [22] A. Amroun *et al.*, *Nucl. Phys.* **A579**, 596 (1994).
- [23] J. Alcorn *et al.*, *Nucl. Instrum. Methods Phys. Res., Sect. A* **522**, 294 (2004).
- [24] S. N. Santiesteban *et al.*, *Nucl. Instrum. Methods Phys. Res., Sect. A* **940**, 351 (2019).
- [25] J. Gao *et al.* (The Jefferson Lab Hall A Collaboration), *Phys. Rev. Lett.* **84**, 3265 (2000).
- [26] J. M. Udias, J. A. Caballero, E. Moya de Guerra, J. E. Amaro, and T. W. Donnelly, *Phys. Rev. Lett.* **83**, 5451 (1999).
- [27] R. Alvarez-Rodriguez, J. M. Udias, J. R. Vignote, E. Garrido, P. Sarriguren, E. Moya de Guerra, E. Pace, A. Kievsky, and G. Salme, *Few Body Syst.* **50**, 359 (2011).
- [28] W. U. Boeglin *et al.* (Hall A Collaboration), *Phys. Rev. Lett.* **107**, 262501 (2011).
- [29] M. M. Sargsian, *Int. J. Mod. Phys. E* **10**, 405 (2001).
- [30] L. L. Frankfurt, M. M. Sargsian, and M. I. Strikman, *Phys. Rev. C* **56**, 1124 (1997).
- [31] S. Jeschonnek and J. W. Van Orden, *Phys. Rev. C* **78**, 014007 (2008).
- [32] J. M. Laget, *Phys. Lett. B* **609**, 49 (2005).
- [33] M. M. Sargsian, *Phys. Rev. C* **82**, 014612 (2010).
- [34] O. Hen, L. B. Weinstein, S. Gilad, and W. Boeglin, arXiv: 1410.4451.
- [35] M. M. Sargsian *et al.*, *J. Phys. G* **29**, R1 (2003).
- [36] R. Cruz-Torres *et al.* (Jefferson Lab Hall A Tritium Collaboration), *Phys. Lett. B* **797**, 134890 (2019).
- [37] E. L. Lomon, arXiv:nucl-th/0609020.
- [38] “SIMC,” https://hallcweb.jlab.org/wiki/index.php/SIMC_Monte_Carlo, 2018.
- [39] C. Carasco *et al.*, *Phys. Lett. B* **559**, 41 (2003).
- [40] J. Bermuth *et al.*, *Phys. Lett. B* **564**, 199 (2003).
- [41] C. Ciofi degli Atti and L. P. Kaptari, *Phys. Rev. C* **71**, 024005 (2005).
- [42] T. De Forest, *Nucl. Phys.* **A392**, 232 (1983).
- [43] R. Machleidt, *Phys. Rev. C* **63**, 024001 (2001).
- [44] R. B. Wiringa, V. G. J. Stoks, and R. Schiavilla, *Phys. Rev. C* **51**, 38 (1995).
- [45] L. E. Marcucci, F. Sammarruca, M. Viviani, and R. Machleidt, *Phys. Rev. C* **99**, 034003 (2019).
- [46] C. Ciofi degli Atti and L. P. Kaptari, *Phys. Rev. Lett.* **95**, 052502 (2005).
- [47] L. Frankfurt, M. Sargsian, and M. Strikman, *Int. J. Mod. Phys. A* **23**, 2991 (2008).
- [48] M. Alvioli, C. Ciofi degli Atti, and L. P. Kaptari, *Phys. Rev. C* **81**, 021001(R) (2010).
- [49] M. Sargsian (private communication).
- [50] M. M. Sargsian, T. V. Abrahamyan, M. I. Strikman, and L. L. Frankfurt, *Phys. Rev. C* **71**, 044614 (2005).
- [51] M. M. Sargsian, T. V. Abrahamyan, M. I. Strikman, and L. L. Frankfurt, *Phys. Rev. C* **71**, 044615 (2005).
- [52] See the Supplemental Material at <http://link.aps.org/supplemental/10.1103/PhysRevLett.124.212501> for additional details on the analysis procedures.
- [53] R. B. Wiringa, R. Schiavilla, S. C. Pieper, and J. Carlson, *Phys. Rev. C* **89**, 024305 (2014).
- [54] O. Hen, G. A. Miller, E. Piasetzky, and L. B. Weinstein, *Rev. Mod. Phys.* **89**, 045002 (2017).
- [55] C. Ciofi degli Atti, *Phys. Rep.* **590**, 1 (2015).
- [56] E. Piasetzky, M. Sargsian, L. Frankfurt, M. Strikman, and J. W. Watson, *Phys. Rev. Lett.* **97**, 162504 (2006).
- [57] R. Subedi *et al.*, *Science* **320**, 1476 (2008).

- [58] I. Korover, N. Muangma, O. Hen *et al.*, *Phys. Rev. Lett.* **113**, 022501 (2014).
- [59] O. Hen *et al.*, *Science* **346**, 614 (2014).
- [60] E. O. Cohen *et al.* (CLAS Collaboration), *Phys. Rev. Lett.* **121**, 092501 (2018).
- [61] M. Duer *et al.* (CLAS Collaboration), *Nature (London)* **560**, 617 (2018).
- [62] M. Duer *et al.* (CLAS Collaboration), *Phys. Rev. Lett.* **122**, 172502 (2019).
- [63] J. R. Pybus, I. Korover, R. Weiss, A. Schmidt, N. Barnea, D. W. Higinbotham, E. Piasetzky, M. Strikman, L. B. Weinstein, and O. Hen, *Phys. Lett. B* **805**, 135429 (2020).
- [64] A. Schmidt *et al.* (CLAS Collaboration), *Nature (London)* **578**, 540 (2020).